arXiv:1410.5546v2 [cond-mat.str-el] 15 Jan 2015

Critical charge fluctuations in a pseudogap Anderson model

Tathagata Chowdhury* and Kevin Ingersent
Department of Physics, University of Florida, P.O. Box 118440, Gainesville, Florida 32611–8440, USA
(Dated: January 16, 2015)

The Anderson impurity model with a density of states $\rho(\varepsilon) \propto |\varepsilon|^r$ containing a power-law pseudogap centered on the Fermi energy ($\varepsilon = 0$) features for $0 < r < 1$ a Kondo-destruction quantum critical point (QCP) separating Kondo-screened and local-moment phases. The observation of mixed valency in quantum critical β-$YbAlB_4$ has prompted study of this model away from particle-hole symmetry. The critical spin response associated with all Kondo destruction QCPs has been shown to be accompanied, for $r = 0.6$ and noninteger occupation of the impurity site, by a divergence of the local charge susceptibility on both sides of the QCP. In this work, we use the numerical renormalization-group method to characterize the Kondo-destruction charge response using five critical exponents, which are found to assume nontrivial values only for $0.55 \lesssim r < 1$. For $0 < r \lesssim 0.55$, by contrast, the local charge susceptibility shows no divergence at the QCP, but rather exhibits nonanalytic corrections to a regular leading behavior. Both the charge critical exponents and the previously obtained spin critical exponents satisfy a set of scaling relations derived from an ansatz for the free energy near the QCP. These critical exponents can all be expressed in terms of just two underlying exponents: the correlation-length exponent $\nu(r)$ and the gap exponent $\Delta(r)$. The ansatz predicts a divergent local charge susceptibility for $\nu < 2$, which coincides closely with the observed range $0.55 \lesssim r < 1$. Many of these results are argued to generalize to interacting QCPs that have been found in other quantum impurity models.

PACS numbers: 71.10.Hf, 71.27.+a, 74.40.Kb, 75.20.Hr

I. INTRODUCTION

Continuous quantum phase transitions (QPTs) in itinerant electron systems are conventionally described within a Ginzburg-Landau-Wilson picture of critical fluctuations of an order parameter characterizing a spontaneously broken symmetry[1–3]. However, experiments on heavy-fermion metals[4] have established the existence of a class of antiferromagnetic quantum critical points (QCPs) that can be understood only by postulating additional critical modes beyond order-parameter fluctuations[5]. It has been proposed[6] that the additional modes arise from the critical destruction of the Kondo effect, associated with a jump in the Fermi-surface volume[7–9] from large in the paramagnetic phase (where unpaired f electrons are absorbed into Kondo resonances) to small in the antiferromagnetic phase (where the Kondo resonances are destroyed and the f electrons are localized).

The picture of critical Kondo destruction was originally developed in the Kondo limit of integer f occupancy. More recently, the discovery of unconventional quantum criticality[10,11] in mixed-valent[12] β-$YbAlB_4$ has prompted interest in critical Kondo destruction at mixed valence. A toy model for this phenomenon is the particle-hole-asymmetric Anderson impurity model with a density of states $\rho(\epsilon) \propto |\epsilon|^r$ that vanishes in power-law fashion on approach to the Fermi energy $\epsilon = 0$. The model features a Kondo-destruction QCP separating a strong-coupling (Kondo-screened) phase from a local-moment (Kondo-destroyed) phase[13–16]. A study conducted using a combination of continuous-time quantum Monte Carlo and the numerical renormalization group (NRG) showed for the particular case $r = 0.6$ that Kondo destruction was accompanied by divergence of a local charge susceptibility on approach to the QCP from either phase[17]. In this case, both spin and charge responses demonstrate the frequency-over-temperature and magnetic field-over-temperature scaling characteristic of an interacting QCP.

This paper extends the numerical results provided in Ref. 17 by determining a complete set of static charge critical exponents for different values of the band exponent r in the range $3/8 \lesssim r < 1$ over which the asymmetric pseudogap Anderson model has an interacting QCP that is distinct from that of its symmetric counterpart[15,16]. We provide a unified description of both the spin and charge critical behaviors in terms of an ansatz for the form of the free energy near the QCP, expressing all critical exponents in terms of just two underlying exponents[18–20], which can be termed (in the nomenclature of classical phase transitions) the "correlation-length" exponent $\nu(r)$ and the "gap" exponent $\Delta(r)$. The ansatz leads to scaling equations that are obeyed to high accuracy by numerically determined values of the charge exponents. In particular, the numerics support a scaling prediction that local charge response is divergent for $\nu < 2$, but regular with nonanalytic corrections for $\nu > 2$.

The outline of the rest of the paper is as follows: Section II defines the pseudogap Anderson Hamiltonian and reviews essential background for the present work. Our numerical results are presented and interpreted in Sec. III. Implications of these results for a broader class of quantum impurity models are discussed in Sec. IV.

II. BACKGROUND

A. Model Hamiltonian

This work addresses an Anderson model described by the Hamiltonian

$$H = \sum_{\mathbf{k},\sigma} \varepsilon_{\mathbf{k}}\, c^\dagger_{\mathbf{k},\sigma} c_{\mathbf{k},\sigma} + \varepsilon_d\, \hat{n}_d + U \hat{n}_{d\uparrow}\, \hat{n}_{d\downarrow} + \frac{V}{\sqrt{N_c}} \big(d^\dagger_\sigma\, c_{\mathbf{k},\sigma} + \text{H.c.} \big) + h \hat{S}_{d,z}, \quad (1)$$

where $c_{\mathbf{k},\sigma}$ (d_σ) destroys a conduction-band (impurity) electron with energy $\varepsilon_{\mathbf{k}}$ (ε_d) and spin z component $\sigma = \pm\frac{1}{2}$ (or $\uparrow, \downarrow$), $\hat{n}_{d\sigma} = d^\dagger_\sigma d_\sigma$ and $\hat{n}_d = \hat{n}_{d\uparrow} + \hat{n}_{d\downarrow}$ are number operators, U is the Coulomb interaction between two electrons within the impurity level (taken to be positive, i.e., repulsive, in our calculations, but see the discussion in Sec. IV), V is the hybridization matrix element between the impurity level and the on-site linear combination of conduction electrons (and is assumed without loss of generality to be real and non-negative), N_c is the number of unit cells in the metallic host and hence the number of distinct values of $\mathbf{k}$, and h is a local magnetic field that couples only to $\hat{S}_{d,z} = \frac{1}{2}(\hat{n}_{d\uparrow} - \hat{n}_{d\downarrow})$, the z component of the impurity spin[21].

The pseudogap variant of the Anderson model has a density of states (per unit cell, per spin z orientation)

$$\rho(\varepsilon) = N_c^{-1} \sum_{\mathbf{k}} \delta(\varepsilon - \varepsilon_{\mathbf{k}}) = \rho_0\, |\varepsilon/D|^r\, \Theta(D - |\varepsilon|), \quad (2)$$

where D is the band half width, and $\Theta(x)$ is the Heaviside function. Values $r > 0$ describe a pseudogapped host, while $r = 0$ corresponds to a conventional metal. If $\rho(\varepsilon)$ has unit normalization, then $\rho_0 = (1 + r)/(2D)$. The values of ρ_0 and V affect the impurity properties only in a single combination, the hybridization width $\Gamma = \pi \rho_0 V^2 \geq 0$.

B. Phase diagram

The phase diagram of the pseudogap Anderson model has been well established by previous work[14,15]. A cut of the phase diagram on the Γ-ε_d plane for a fixed value of $U > 0$ is shown schematically for $0 < r < \frac{1}{2}$ in Fig. 1(a) and for $r \geq \frac{1}{2}$ in Fig. 1(b).

In the metallic case $r = 0$, for all finite values of U and ε_d and for any $\Gamma > 0$, the impurity degree of freedom is completely quenched in the limit of absolute temperature $T \to 0$, and a single strong-coupling (SC) phase occupies the entire half space (U, ε_d, Γ) apart from its boundary plane $\Gamma = 0$. Throughout this phase, the impurity contributions to the static spin susceptibility and the entropy satisfy $\lim_{T\to 0} T\chi_{\text{imp}} = 0$ and $S_{\text{imp}}(T = 0) = 0$, respectively[21]. The ground-state "charge" Q, defined to be the expectation value of the total electron occupancy of the band and the impurity level measured with respect to half filling, evolves smoothly from 1 to -1 as ε_d is raised from $-\infty$ to ∞.

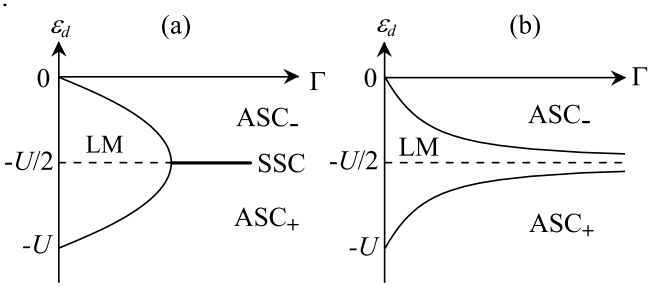

FIG. 1. Schematic phase diagram of the pseudogap Anderson model on the Γ-ε_d plane for fixed U and for band exponents (a) $0 < r < \frac{1}{2}$, and (b) $r \geq \frac{1}{2}$. In (a), the SSC phase spans just the solid horizontal line at $\varepsilon_d = -U/2$.

For $r > 0$, by contrast, there is local-moment (LM) phase spanning $-U < \varepsilon_d < 0$, $\Gamma < \Gamma_c(U, \varepsilon_d) \equiv \Gamma_c(U, -U - \varepsilon_d)$ within which the ground state contains an unquenched spin degree of freedom characterized by $\lim_{T\to 0} T\chi_{\text{imp}} = 1/4$ and $S_{\text{imp}}(T = 0) = \ln 2$. For $\Gamma > \Gamma_c(U, \varepsilon_d)$, the system lies in one of three SC phases. The symmetric strong-coupling (SSC) phase, reached only for $\varepsilon_d = -U/2$ [see solid horizontal line in Fig. 1(a)], has $\lim_{T\to 0} T\chi_{\text{imp}} = r/8$ and $S_{\text{imp}}(T = 0) = 2r \ln 2$, suggestive of partial quenching of the impurity spin. The asymmetric strong-coupling phases ASC$_-$ and ASC$_+$, reached for $\varepsilon_d > -U/2$ and $\varepsilon_d < -U/2$, respectively, share the properties $\lim_{T\to 0} T\chi_{\text{imp}} = 0$ and $S_{\text{imp}}(T = 0) = 0$, indicating complete quenching of the impurity degree of freedom. For $r > 0$, the ground-state charge takes only integer values (in contrast to the case $r = 0$): $Q = 0$ in the LM and SSC phases, $Q = \pm 1$ in the ASC$_\pm$ phase.

It should be noted that the SSC phase can be reached only for $0 < r < \frac{1}{2}$, on which range $\Gamma_c(U, -U/2)$ is finite [see Fig. 1(a)]. For $r \geq \frac{1}{2}$, the SSC ground state is unstable, and $\Gamma_c(U, \varepsilon_d)$ diverges as $\varepsilon_d \to -U/2$ from above or below, so for $\varepsilon_d = -U/2$ the system always lies in the LM phase [see Fig. 1(b)].

C. Critical spin response

On the boundary between the LM and SC phases, the thermodynamic properties take values distinct from those in either phase. For example, $\lim_{T\to 0} T\chi_{\text{imp}}(T) = X(r)$, where $r/8 < X(r) < 1/4$ (see Fig. 14 of Ref. 15). However, the nontrivial critical properties of the pseudogap Anderson model (and of the pseudogap Kondo model to which the Anderson model reduces when charge fluctuations on the impurity site can be neglected) are revealed more clearly in the response to a local magnetic field that acts solely at the impurity spin[16,18], as represented by h entering Eq. (1). This response is measured

by the zero-temperature local magnetization

$$M_{\rm loc} = -\partial F_{\rm imp}/\partial h|_{T=0} = -\langle \hat{S}_{d,z}\rangle|_{T=0} \tag{3}$$

and the zero-field local spin susceptibility

$$\chi_s = -\partial^2 F_{\rm imp}/\partial h^2|_{h=0} = -\partial\langle \hat{S}_{d,z}\rangle/\partial h|_{h=0}, \tag{4}$$

where $F_{\rm imp}$ is the impurity contribution to the system's free energy. The value of $M_{\rm loc}$ in an infinitesimal symmetry-breaking field $h = 0^+$ is nonzero in the LM phase ($\Gamma < \Gamma_c$) but zero in the SC phases ($\Gamma > \Gamma_c$), and therefore serves as an order parameter for the LM-SC QPT, while the zero-temperature limit of χ_s diverges on approach to the QPT from the SC side and is infinite throughout the LM phase.

For $r > 1$, $M_{\rm loc}$ is discontinuous across the phase boundaries, meaning that the QPTs are first order. For $0 < r < 1$, by contrast, the QPTs are continuous and the local magnetic critical behavior can be characterized by a set of critical exponents β, γ, δ, and x defined through the relations[18,20]

$$M_{\rm loc}(g \le 0, h = 0^+) \propto (-g)^{\beta}, \tag{5a}$$

$$|M_{\rm loc}(g = 0)| \propto |h|^{1/\delta}, \tag{5b}$$

$$\chi_s(T = 0, g > 0) \propto g^{-\gamma}, \tag{5c}$$

$$\chi_s(g = 0) \propto T^{-x}, \tag{5d}$$

where one can define the nonmagnetic distance to criticality to be $g = \Gamma - \Gamma_0$ at fixed $U = U_0$ and $\varepsilon_d = \varepsilon_{d0}$ or, alternatively, $g = U_0 - U$ at fixed $\Gamma = \Gamma_0$ and $\varepsilon_d = \varepsilon_{d0}$, where in either case $\Gamma_0 = \Gamma_c(U_0, \varepsilon_{d0})$. One can also define a correlation-length exponent ν via the relation

$$T^* \propto |g|^{\nu}, \tag{6}$$

where T^* is a temperature characterizing the crossover from the quantum-critical regime ($\chi_s \propto T^{-x}$ for $T \gg T^*$) to either the LM phase ($\chi_s \propto T^{-1}$ for $g < 0$, $T \ll T^*$) or one of the SC phases ($\chi_s \simeq$ const for $g > 0$, $T \ll T^*$). Each of the critical exponents β, γ, δ, x, and ν has a nontrivial dependence[18] on the band exponent r.

For $0 < r \le r^* \simeq 3/8$, it is found[18] that the critical exponents take identical values all the way along the phase boundary between the LM and SC phases. Specifically, particle-hole asymmetry is irrelevant along the boundary and the QPT is governed by a symmetric QCP. For $r \ge \frac{1}{2}$, there is no QPT at particle-hole symmetry; a single asymmetric QCP governs the LM-ASC$_-$ boundary, while a second QCP (related to the first by a particle-hole transformation, and sharing the same set of critical exponents) governs the LM-ASC$_+$ boundary. Over the range $r^* < r < \frac{1}{2}$, there is coexistence of symmetric and asymmetric QCPs, which have different critical exponents for a given band exponent r.

Over the entire range $0 < r < 1$, the critical exponents (for both symmetric and asymmetric QCPs) obey a set of scaling relations[18],

$$\beta = \nu(1-x)/2, \quad \gamma = \nu x, \quad 1/\delta = (1-x)/(1+x), \tag{7}$$

that are consistent with a scaling ansatz for the critical part of the free energy,

$$F_{\rm imp}^{\rm crit} = T f\left(\frac{g}{T^{1/\nu}}, \frac{|h|}{T^{\Delta/\nu}}\right), \tag{8}$$

written in terms of just two underlying critical exponents, ν defined in Eq. (6) and the gap exponent Δ. This scaling form, which is expected to hold only for an interacting QCP below its upper critical dimension, implies that

$$\beta = \nu - \Delta\,, \tag{9a}$$

$$\gamma = 2\Delta - \nu\,, \tag{9b}$$

$$1/\delta = \nu/\Delta - 1\,, \tag{9c}$$

$$x = 2\Delta/\nu - 1\,. \tag{9d}$$

Elimination of Δ from Eqs. (9) yields Eqs. (7).

D. Critical charge response

Reference 17 investigated local charge fluctuations in the vicinity of the Kondo-destruction QPTs in the pseudogap Anderson model. The local charge response is the variation of the impurity charge $\hat{n}_d$, which enters the Hamiltonian with coupling ε_d, so it is natural to define a local charge susceptibility

$$\chi_c = -\partial\langle \hat{n}_d\rangle/\partial\varepsilon_d|_{\varepsilon_d=\varepsilon_{d0}}, \tag{10}$$

near a point $(U_0, \varepsilon_{d0}, \Gamma_0)$ on the phase boundary. It was reported in Ref. 17 that χ_c remains finite on passage through the particle-hole-symmetric QCPs that occur for $0 < r < \frac{1}{2}$. However, it was shown for the specific case $r = 0.6$ that χ_c diverges on approach to the LM-ASC$_\pm$ boundary from either phase. The behavior for this particular band exponent was found to be described by a pair of critical exponents $\tilde{\gamma}$, and $\tilde{x}$ defined via the relations

$$\chi_c(T = h = 0) \propto |g|^{-\tilde{\gamma}}, \tag{11a}$$

$$\chi_c(g = h = 0) \propto T^{-\tilde{x}}, \tag{11b}$$

where $g = U_0 - U$ at fixed $\varepsilon_d = \varepsilon_{d0}$ and $\Gamma = \Gamma_0 = \Gamma_c(U_0, \varepsilon_{d0})$. Equation (11a) differs from Eq. (5c) in that $\chi_c(T = 0)$ remains finite for all $g < 0$ as well as for all $g > 0$.

III. RESULTS AND INTERPRETATION

We have systematically extended the results of Ref. 17 through study of the particle-hole-asymmetric pseudogap Anderson model with different values of the band exponent r within the range $r^* < r < 1$. We have departed from Ref. 17 in that for the most part we have fixed U and varied ε_d and Γ, so that we have extracted $\tilde{\gamma}$ and $\tilde{x}$ defined through Eqs. (11) using $g = \Gamma - \Gamma_0$ at fixed $U = U_0$ and $\varepsilon_d = \varepsilon_{d0}$. For any given r, variation of U

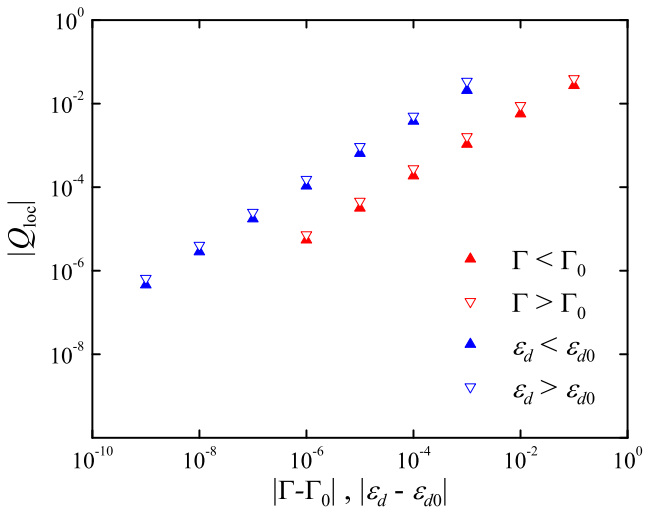

FIG. 2. (Color online) $|Q_{\rm loc}|$ vs distance from the phase boundary along the Γ and ε_d axes for $r = 0.6$. Filled (hollow) symbols represent points in the LM (ASC$_-$) phase. The linear variations on this log-log plot indicate power-law behavior in accordance with Eqs. (13).

and variation of Γ are found to yield the same numerical values of these critical exponents and of other exponents defined below.

In addition to calculating χ_c, we have also investigated the variation of the impurity occupancy near the QCP. Since $\langle \hat{n}_d \rangle$ is not pinned to any fixed value throughout either the LM phase or the ASC$_\pm$ phases, it does not act like an order parameter. It proves convenient to define a zero-temperature local charge

$$Q_{\rm loc} = \langle \hat{n}_d(U, \varepsilon_d, \Gamma) - \hat{n}_d(U_0, \varepsilon_{d0}, \Gamma_0) \rangle|_{T=0}, \qquad (12)$$

constructed to vanish at the point $(U_0, \varepsilon_{d0}, \Gamma_0)$ where the phase boundary is crossed.

We have calculated $Q_{\rm loc}$ and $\chi_c = \lim_{\varepsilon_d \to \varepsilon_{d0}} Q_{\rm loc}/(\varepsilon_{d0} - \varepsilon_d)$ using the numerical renormalization-group (NRG) method, as adapted to treat pseudogapped densities of states[15]. We have employed a discretization parameter $\Lambda = 9$, shown in previous NRG studies of the pseudogap Kondo[18] and Anderson[17] models to yield critical exponents very close to their values in the continuum limit $\Lambda \to 1$, and retained up to 600 many-body eigenstates after each NRG iteration. All results[21] shown below are for a representative point on the LM-ASC$_-$ phase boundary at $U_0 = 0.1D$, $\varepsilon_{d0} = -0.03D$, and $\Gamma_0 = \Gamma_c(U_0, \varepsilon_{d0})$. However, other runs indicate that exponents depend on r but not on the specific values of U_0, ε_{d0}, and Γ_0 (provided that $\varepsilon_{d0} \neq -U_0/2$).

Figure 2 illustrates the variation of $Q_{\rm loc}$ for the case $r = 0.6$. Irrespective of from which side the LM-ASC$_-$ boundary is approached, $Q_{\rm loc}$ displays power-law variation over six decades of $|\Gamma - \Gamma_0|$ at $\varepsilon_d = \varepsilon_{d0}$ and over five decades of $|\varepsilon_d - \varepsilon_{d0}|$ at $\Gamma = \Gamma_0$. It should be noted that these power laws reveal themselves in both phases (unlike the power-law variation of $M_{\rm loc}$, which occurs only on the LM side of the QCP). The parallel trends of the data on this log-log plot suggest that variation of $Q_{\rm loc}$ with respect to Γ and with respect to ε_d is governed by a common critical exponent $\tilde{\beta}$, i.e.,

$$|Q_{\rm loc}(\varepsilon_d = \varepsilon_{d0})| \propto |g|^{\tilde{\beta}}, \qquad (13a)$$

$$|Q_{\rm loc}(g = 0)| \propto |\varepsilon_d - \varepsilon_{d0}|^{\tilde{\beta}}. \qquad (13b)$$

This supposition is confirmed in Fig. 3(a), which plots values of $\tilde{\beta}$ obtained from Eqs. (13a) and (13b) for different band exponents over the range $0.4 \leq r \leq 0.9$. For $r < 0.4$, it proves very difficult to distinguish the symmetric and asymmetric QCPs (which merge at $r = r^* \simeq 0.375$), while for $r \geq 0.9$ power laws tend to become ill-defined as the system nears its upper critical dimension[16] at $r = 1$. The other striking feature of Fig. 3(a) is the sharp break around $r = 0.55$ between the pinned value $\tilde{\beta} = 1$ for $r \lesssim 0.55$ and the monotonic decrease of $\tilde{\beta}$ over the range $0.55 \lesssim r < 1$. This decrease of $\tilde{\beta}$ points to a variation of the impurity valence around the QCP that becomes more rapid with increasing r and presumably becomes discontinuous for $r > 1$.

The r dependencies of the critical exponents $\tilde{x}$ and $\tilde{\gamma}$ characterizing the local charge susceptibility are plotted in Figs. 3(b) and 3(c), respectively. Each of these exponents is positive for $r \gtrsim 0.55$, while it appears to vanish for $r \lesssim 0.55$.

Table I summarizes the numerical values of the three charge critical exponents defined in Eqs. (11) and (13) and of ν, the correlation-length exponent. Also listed is an estimate of the non systematic error in the last decimal place of each exponent. Exponent $\tilde{x}$ from Eq. (11b) generally has the smallest error because it can be obtained from fits of $\chi_{\rm loc}$ over many decades of T. There is considerable uncertainty in the values of ν, which were obtained by interpolating from data at discrete temperatures T the

r	$\tilde{\beta}$ (13a)	$\tilde{\beta}$ (13b)	$\tilde{\gamma}$	$\tilde{x}$	ν
0.40	1.000(2)	1.000(1)		0.0000(1)	4.24(4)
0.50	1.000(3)	1.000(2)		0.0000(2)	2.36(4)
0.52		1.000(4)		0.0000(2)	2.22(3)
0.54		0.997(4)		0.000(1)	2.08(3)
0.56		0.965(6)		0.021(1)	1.98(4)
0.58		0.876(5)		0.0658(6)	1.88(4)
0.60	0.7910(6)	0.7913(5)	0.210(2)	0.1164(1)	1.77(4)
0.70	0.472(4)	0.474(4)	0.524(4)	0.3569(4)	1.45(3)
0.80	0.263(2)	0.265(2)	0.728(8)	0.582(2)	1.29(4)
0.90	0.109(4)	0.105(5)	0.872(2)	0.790(2)	1.13(6)

TABLE I. Charge critical exponents $\tilde{\beta}$, $\tilde{\gamma}$, and $\tilde{x}$, plus correlation-length exponent ν, at the particle-hole-asymmetric QCPs of the pseudogap Anderson model for band exponents r between 0.4 and 0.9. Exponent $\tilde{\beta}$ was obtained independently from fits to Eqs. (13a) and (13b). Parentheses enclose the estimated nonsystematic error in the last digit. Each charge critical exponent agrees to within its estimated error with the value obtained by substituting ν into the appropriate scaling relation in Eqs. (17).

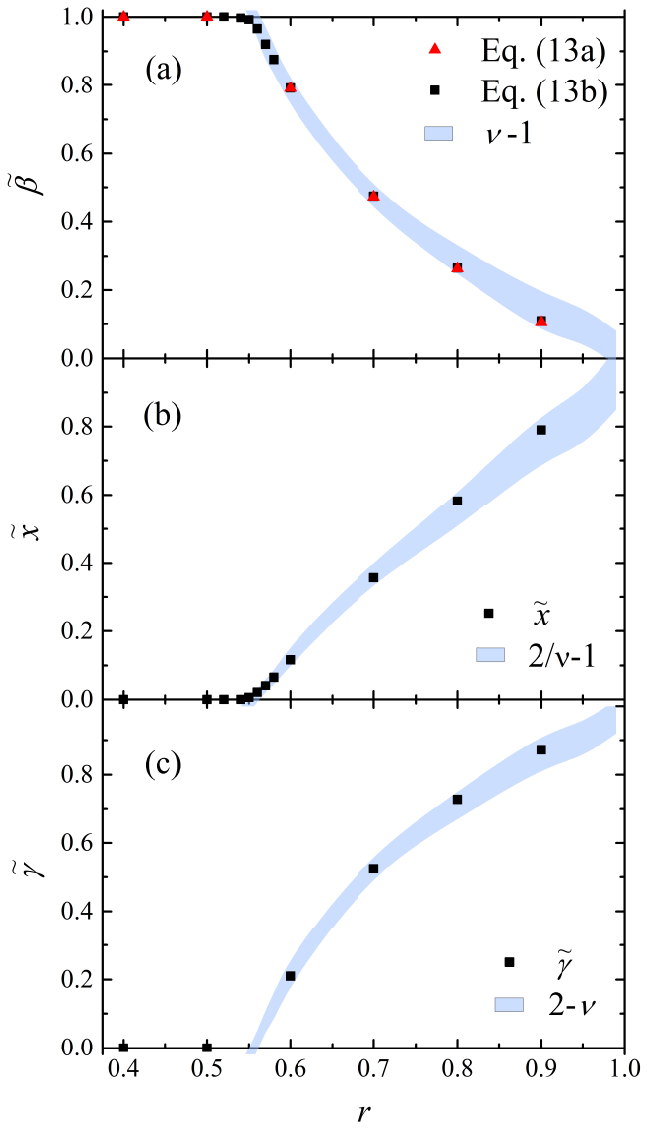

FIG. 3. (Color online) Charge critical exponents plotted vs pseudogap exponent r: (a) $\tilde{\beta}$ obtained independently from the variation of $Q_{\rm loc}$ with respect to ε_d and with respect to Γ, (b) $\tilde{x}$, and (c) $\tilde{\gamma}$. In all cases, the estimated nonsystematic error is smaller than the data symbol. Shading indicates the range within which each exponent is predicted to lie when the values of the correlation-length exponent ν from Table I are inserted into Eqs. (17).

value T^* at which $T\chi_{\rm imp}(T)$ passes outside a narrow window surrounding its critical value $X(r)$. When allowance is made for these uncertainties, Table I suggests an interesting relation among the charge critical exponents, namely,

$$\tilde{\beta} = 1 - \tilde{\gamma}. \tag{14}$$

Finally, we note that the threshold value of the band exponent $r \simeq 0.55$ seems to coincide with the point where the correlation-length exponent passes through $\nu = 2$.

Many of the empirical observations noted in the preceding paragraphs can be understood through an extension of the scaling ansatz used previously[18] to explain the critical spin response. We postulate that the singular component of the impurity free energy takes the form given in Eq. (8) with a generalized definition of the nonmagnetic distance from criticality, namely,

$$g = (\mathbf{p} - \mathbf{p}_0) \cdot \hat{\mathbf{n}}_0. \tag{15}$$

Here, $\hat{\mathbf{n}}_0$ is the local unit normal to the phase boundary at $\mathbf{p}_0 = (U_0, \varepsilon_{d0}, \Gamma_0)$, $h = 0$ in a three-dimensional Euclidean space of nonmagnetic couplings $\mathbf{p} = (U, \varepsilon_d, \Gamma)$; the direction of $\hat{\mathbf{n}}_0$ is chosen so that it points into the SC phase. This form is assumed to hold for $|\mathbf{p} - \mathbf{p}_0|$ much smaller than the radii of curvature of the phase boundary at $\mathbf{p}_0$, in which case $|g|$ is just the perpendicular distance from $\mathbf{p}$ to the phase boundary.

The extended ansatz reproduces the critical spin response in Eqs. (5) with exponents satisfying Eqs. (7), irrespective of whether the approach to the phase boundary is along the U, ε_d, or Γ axis (or along any direction in between). The ansatz also recovers the critical charge response[22] in Eqs. (11) and (13), as well as two further power-law behaviors,

$$Q_{\rm loc}(g = 0) \propto |h|^{1/\tilde{\delta}}, \tag{16a}$$

$$\chi_c(T = g = 0) \propto |h|^{-\tilde{\phi}}, \tag{16b}$$

with all critical exponents expressed as functions of ν and Δ:

$$\tilde{\beta} = \nu - 1, \tag{17a}$$

$$\tilde{\gamma} = 2 - \nu, \tag{17b}$$

$$\tilde{x} = 2/\nu - 1, \tag{17c}$$

$$1/\tilde{\delta} = (\nu - 1)/\Delta, \tag{17d}$$

$$\tilde{\phi} = (2 - \nu)/\Delta. \tag{17e}$$

Equations (17a) and (17b) not only confirm Eqs. (14), but also show that since the local "field" ε_d conjugate to the local charge enters the free energy in the same manner as do U and Γ, the charge critical exponents $\tilde{\beta}$, $\tilde{\gamma}$, and $\tilde{x}$ are functions solely of ν, unlike their spin counterparts β, γ, and x, which also depend on Δ.

For all cases studied on the range $0.55 \lesssim r \leq 0.9$, the directly determined exponents $\tilde{\beta}$, $\tilde{x}$, and $\tilde{\gamma}$ lie within the bounds (represented by shaded regions in Fig. 3) obtained by inserting numerical estimates of ν into Eqs. (17). Given the rather large uncertainties in ν, a more rigorous test of the scaling relations is provided by Table II, which compares the directly determined value of ν for $0.6 \leq r \leq 0.9$ with ones inferred through the scaling relations from the NRG values of $\tilde{\beta}$, $\tilde{x}$, and $\tilde{\gamma}$. For each band exponent $r \leq 0.8$, all values of ν agree to within their estimated nonsystematic errors, providing strong numerical support for the validity of Eqs. (17). We attribute the discrepancies between the various estimates of ν for

r	ν	ν found from			
	direct	$\tilde{\beta}$ (13a)	$\tilde{\beta}$ (13b)	$\tilde{\gamma}$	$\tilde{x}$
0.6	1.77(4)	1.7910(6)	1.7913(5)	1.790(2)	1.7915(6)
0.7	1.45(3)	1.472(4)	1.474(2)	1.476(4)	1.474(1)
0.8	1.29(4)	1.263(2)	1.265(2)	1.272(8)	1.264(2)
0.9	1.13(6)	1.109(4)	1.105(5)	1.128(2)	1.117(2)

TABLE II. Correlation-length exponent ν at the particle-hole-asymmetric QCPs of the pseudogap Anderson model for band exponents r between 0.6 and 0.9, as obtained directly and via the scaling equations (17) from the charge critical exponents listed in Table I. Except for $r = 0.9$, the various estimates of ν for a given r all agree to within the estimated nonsystematic error in the last digit of each value (enclosed in parentheses).

r	$1/\tilde{\delta}$ (dir.)	$1/\tilde{\delta}$ (17d)	$\tilde{\phi}$ (dir.)	$\tilde{\phi}$ (17e)	x
0.6	0.4941(5)	0.4934(2)	0.1306(6)	0.1300(2)	0.79057(6)
0.7	0.3517(3)	0.3512(6)	0.393(3)	0.390(1)	0.8315(1)
0.8	0.2240(7)	0.222(2)	0.620(6)	0.619(3)	0.88021(7)
0.9	0.130(6)	0.109(3)	0.80(2)	0.820(4)	0.928(2)

TABLE III. Exponents $\tilde{\delta}$ and $\tilde{\phi}$ as determined directly ("dir.") from Eqs. (16) for band exponents r between 0.6 and 0.9. Also listed are values of the same exponents inferred from scaling equations Eqs. (17d) and (17e), respectively, using the best estimate of ν from Table II and a value of Δ found via Eq. (9d) from the tabulated value of the magnetic exponent x. Except for $r = 0.9$, the directly determined and inferred exponents agree to within the estimated nonsystematic error in the last digit of each value (enclosed in parentheses).

$r = 0.9$ to the difficulty mentioned above in identifying clear power-law behaviors for band exponents approaching 1.

Table III lists, for band exponents $0.6 \leq r \leq 0.9$, directly computed values of the exponents $1/\tilde{\delta}$ and $\tilde{\phi}$ defined in Eqs. (16) as well the values of the same exponents predicted from scaling Eqs. (17d) and (17e), respectively. For $r = 0.9$, it proved difficult to obtain a robust power-law variation of $Q_{\rm loc}$ with h, so no directly computed value is recorded for $1/\tilde{\delta}$. The inputs to the scaling equations are (i) the value of the correlation-length exponent ν found from $\tilde{x}$ using Eq. (17c) (see rightmost column of Table II), and (ii) a value of the gap exponent Δ found via Eq. (9d) from the magnetic exponent x. The values of x (also listed in Table III) are either directly computed in the Anderson model (for $r = 0.7$) or obtained by refining previous results[18] for the pseudogap Kondo model. That the directly computed values in all cases but one ($1/\tilde{\delta}$ for $r = 0.9$) agree with their scaling predictions to within the estimated nonsystematic errors further supports the validity of the extended scaling ansatz contained in Eqs. (8) and (15).

The extended scaling ansatz has implications not only for relations among critical exponents but also for the relative magnitude of responses at different points $\mathbf{p}$ near $\mathbf{p}_0$. NRG runs performed for fixed $|\mathbf{p} - \mathbf{p}_0|$ but for various angles between $\mathbf{p} - \mathbf{p}_0$ and the local normal $\hat{\mathbf{n}}_0$ are consistent with the hypothesis that local spin and charge properties depend only on g as defined in Eq. (15).

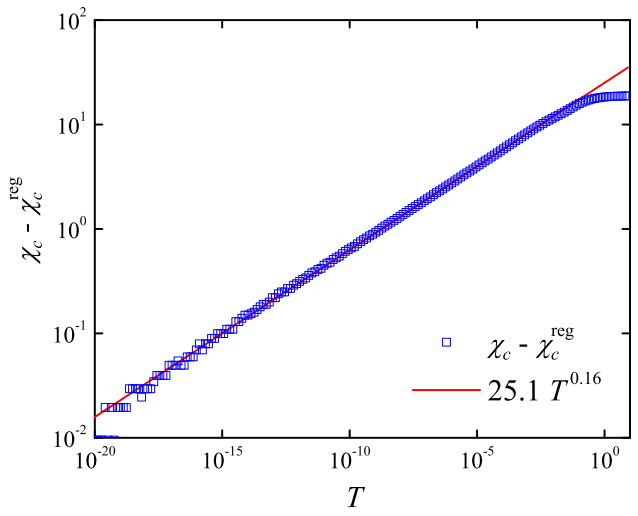

FIG. 4. (Color online) Temperature-dependent part $\chi_c - \chi_c^{\rm reg}$ of the local charge susceptibility for band exponent $r = 0.5$. The line fitted through the NRG data points corresponds to $\chi_c - \chi_c^{\rm reg} \propto T^{0.16}$.

For $r \lesssim 0.55$ (which is the range in which $\nu > 2$), the scaling relations in Eqs. (17) predict that $\tilde{\beta} > 1$ and $\tilde{x}, \tilde{\gamma} < 0$. In contrast, we find numerically that $\tilde{\beta}$, $\tilde{x}$, and $\tilde{\gamma}$ are pinned at trivial values of 1, 0, and 0 respectively. In order to explain the strong deviations from scaling over this range of band exponents, it turns out to be essential to consider the hitherto neglected regular (analytic) parts,

$$F_{\rm imp}^{\rm reg} = -\frac{1}{2}\,\chi_c^{\rm reg}\,g^2 - \frac{1}{2}\,\chi_s^{\rm reg}\,h^2 + \ldots, \qquad (18)$$

of the total impurity free energy $F_{\rm imp} = F_{\rm imp}^{\rm crit} + F_{\rm imp}^{\rm reg}$. The regular terms impart a piece to $Q_{\rm loc}$ varying linearly with g (i.e., $\tilde{\beta} = 1$) and a constant local charge susceptibility (formally corresponding to $\tilde{x} = \tilde{\gamma} = 0$). For any $\nu > 2$, these contributions dominate the charge responses described by Eqs. (17) that arise from the critical part of the free energy. The condition $\nu > 2$ does not preclude a divergent local spin susceptibility, which depends not only on ν but also the gap exponent Δ. Indeed, nontrivial critical behavior in the spin sector persists for $r \to 0^+$, in which limit there is a divergent correlation-length exponent $\nu \simeq 1/r$ (Refs. 16 and 23).

It should be pointed out that a nonanalytic charge response, albeit subleading, is still present in the range of band exponents where $\nu > 2$. This is illustrated in Fig. 4, a log-log plot of $\chi_c(T) - \chi_c^{\rm reg}$ [where $\chi_c^{\rm reg} \equiv \chi_c(T \to 0)$] versus temperature for the representative case $r = 0.5$. An empirical fit $\chi_c - \chi_c^{\rm reg} \propto T^{0.16}$ is in close agreement with the expectation based on Eq. (17c) of a temperature exponent $1 - 2/\nu = 0.15(3)$.

IV. DISCUSSION

This work has shed light on the critical local charge response found previously near the Kondo-destruction quantum critical point (QCP) in the pseudogap Anderson impurity model away from particle-hole symmetry[17]. The "field" conjugate to the local charge (i.e., the impurity occupancy) is the impurity level energy ε_d. Changing ε_d does not destroy or restore the SU(2) spin-rotation invariance that distinguishes the model's strong-coupling phase from its broken-symmetry local-moment phase. For this reason, ε_d joins other model couplings, such as the interaction strength U and the hybridization width Γ, whose collective deviation g from the phase boundary enters an ansatz [Eq. (8)] for the free energy in the scaling combination $g/T^{1/\nu}$, distinct from the $|h|/T^{\Delta/\nu}$ scaling of the local magnetic field[24]. First and second partial derivatives of the free-energy with respect to ε_d exhibit power-law variations with exponents $\tilde{\beta}$, $\tilde{\gamma}$, $\tilde{\delta}$, $\tilde{\phi}$, and $\tilde{x}$ that depend on ν, but (apart from $\tilde{\delta}$ and $\tilde{\phi}$) are independent of Δ. Presumably, the corresponding partial derivatives of the free energy with respect to U and Γ would be described by the same set of exponents.

In all cases studied numerically in this work, the local charge response at the QCP has proved to be less singular than the local spin response. However, it is straightforward to come up with an example where the reverse ordering holds. Interchange of spin and charge degrees of freedom maps the $U > 0$ Anderson model in zero magnetic field to a $U < 0$ Anderson model at particle-hole symmetry. In the presence of a pseudogapped density of states described by exponent $0 < r < 1$, this negative-U Anderson model must have a QCP between strong-coupling and local-charge phases[25] at which the local charge response is governed by critical exponents β, γ, δ, and x, while the local spin response is weaker and described by critical exponents $\tilde{\beta}$, $\tilde{\gamma}$, $\tilde{\delta}$, $\tilde{\phi}$, and $\tilde{x}$.

What does seem intuitively reasonable is that the response to the order-parameter field is more singular than that to other perturbations of the system. Indeed, one can argue that this should be true at any interacting QCP described by the scaling ansatz Eq. (8), examples of which have been identified in a number of other quantum impurity models[19,26–30]. At such a QCP, the response to the order-parameter field will be the most singular response provided that the gap exponent satisfies $\Delta > 1$, a condition that can be shown using Eqs. (7) and (9d) [all derived from Eq. (8)] to be equivalent to $\beta + \gamma > 1$. Since any interacting QCP is expected to satisfy $\beta > 0$ (describing a continuous power-law rise of the order parameter) and $\gamma \geq 1$ ($\gamma = 1$ being the mean-field value), $\beta + \gamma > 1$ should be satisfied quite generally.

In summary, we have provided a unified picture of critical spin and charge responses at quantum critical points in the particle-hole-asymmetric pseudogap Anderson Hamiltonian, a toy model for investigating critical Kondo destruction at mixed valence. All critical exponents have been related to just two underlying exponents: the correlation-length exponent ν and the gap exponent Δ. The charge susceptibility diverges at the transition provided $\nu < 2$, while for $\nu > 2$ the local charge response is regular with nonanalytic corrections. We have argued that nonanalytic responses to non-symmetry-breaking fields are a generic feature of interacting QCPs in quantum impurity models, although such responses should be less singular than those to a field breaking the symmetry that distinguishes the phases on either side of the QCP.

V. ACKNOWLEDGMENTS

We acknowledge useful conversations with J. Pixley and Q. Si. This work has been supported by NSF Grant No. DMR-1107814.

* Electronic address: tatha@phys.ufl.edu

1. J. A. Hertz, Phys. Rev. B **14**, 1165 (1976).
2. A. J. Millis, Phys. Rev. B **48**, 7183, (1993).
3. S. Sachdev, *Quantum Phase Transitions* (Cambridge University Press, Cambridge, UK, 1999).
4. For reviews, see H. v. Löhneysen, A. Rosch, M. Vojta, and P. Wölfe, Rev. Mod. Phys. **79**, 1015, (2007); Q. Si and F. Steglich, Science **329**, 1161 (2010).
5. P. Coleman, C. Pépin, Q. Si, and R. Ramazashvili, J. Phys.: Condens. Matter **13**, R723 (2001).
6. Q. Si, S. Rabello, K. Ingersent, and J. L. Smith, Nature (London) **413**, 804 (2001); Phys. Rev. B **68**, 115103 (2003).
7. S. Paschen, T. Lühmann, S. Wirth, P. Gegenwart, O. Trovarelli, C. Geibel, F. Steglich, P. Coleman, and Q. Si, Nature (London) **432**, 881 (2004);
8. H. Shishido, R. Settai, H. Harima, and Y. Onuki, J. Phys. Soc. Jpn. **74**, 1103 (2005).
9. S. Friedemann, N. Oeschler, S. Wirth, C. Krellner, C. Geibel, F. Steglich, S. Kirchner, and Q. Si, Proc. Natl. Acad. Sci. U.S.A. **107**, 14547 (2010).
10. S. Nakatsuji *et al.*, Nat. Phys. **4**, 603 (2008).
11. Y. Matsumoto, S. Nakatsuji, K. Kuga, Y. Karaki, N. Horie, Y. Shimura, T. Sakakibara, A. H. Nevidomskyy, and P. Coleman, Science **331**, 316 (2011).
12. M. Okawa *et al.*, Phys. Rev. Lett. **104**, 247201 (2010).
13. C. Gonzalez-Buxton and K. Ingersent, Phys. Rev. B **54**, 15614 (1996).
14. R. Bulla, Th. Pruschke, and A. C. Hewson, J. Phys.: Condens. Matter **9**, 10463 (1997).
15. C. Gonzalez-Buxton and K. Ingersent, Phys. Rev. B **57**, 14254 (1998).
16. L. Fritz and M. Vojta, Phys. Rev. B **70**, 214427 (2004).
17. J. H. Pixley, S. Kirchner, K. Ingersent, and Q. Si, Phys. Rev. Lett. **109**, 086403 (2012).
18. K. Ingersent and Q. Si, Phys. Rev. Lett. **89**, 076403 (2002).

[19] M. Vojta, Philos. Mag. **86**, 1807 (2006).
[20] In the literature on impurity quantum phase transitions, Δ/ν is usually written as $(1+x)/2$ or $1-\eta/2$, where $\eta = 1-x \geq 0$ is the anomalous magnetic exponent.
[21] We work in units where $g\mu_B = k_B = \hbar = 1$.
[22] With g as defined in Eq. (15), Eq. (13b) becomes a special case of Eq. (13a).
[23] M. Kirćan and M. Vojta, Phys. Rev. B **69**, 174421 (2004).
[24] In the limit of unit impurity occupancy, the pseudogap Anderson model can be mapped at low energies to a pseudogap Kondo model with an exchange coupling J and a potential scattering V. In this Kondo model, we expect that the critical part of the impurity free energy satisfies the scaling ansatz in Eq. (8) with $|g|$ being the length of the perpendicular to the phase boundary [parametrized as $J_0 = J_c(V_0)$] that passes through the point (J, V) representing the bare model parameters.
[25] The presence of a QCP between strong-coupling and local-charge phases, with a local charge response governed by critical exponents identical to the spin exponents of the pseudogap Anderson model, has been shown explicitly for the pseudogap Anderson-Holstein model, where a coupling of the impurity charge to a local bosonic degree of freedom gives rise to an effective on-site attraction $U_{\rm eff} < 0$; see M. Cheng and K. Ingersent, Phys. Rev. B **87**, 075145 (2013).
[26] M. Vojta, N.-H. Tong, and R. Bulla, Phys. Rev. Lett. **94**, 070604 (2005).
[27] M. T. Glossop and K. Ingersent, Phys. Rev. Lett. **95**, 067202 (2005); Phys. Rev. B **75**, 104410 (2007).
[28] C.-H. Chung, M. T. Glossop, L. Fritz, M. Kircan, K. Ingersent, and M. Vojta, Phys. Rev. B **76**, 235103 (2007).
[29] M. Cheng, M. T. Glossop, and K. Ingersent, Phys. Rev. B **80**, 165113 (2009).
[30] J. H. Pixley, S. Kirchner, K. Ingersent, and Q. Si, Phys. Rev. B **88**, 245111 (2013).